PHYSICAL REVIEW B **91**, 161404(R) (2015)

Strain-induced metal-semiconductor transition in monolayers and bilayers of gray arsenic: A computational study

Zhen Zhu, Jie Guan, and David Tománek*

Physics and Astronomy Department, Michigan State University, East Lansing, Michigan 48824, USA

(Received 2 October 2014; published 9 April 2015)

We study the equilibrium geometry and electronic structure of thin films of layered gray arsenic using *ab initio* density functional theory. In contrast to bulk gray As that is semimetallic, thin films display a significant band gap that depends sensitively on the number of layers, in-layer strain, layer stacking, and interlayer spacing. We find that metallic character can be introduced by increasing the number of layers beyond two or by subjecting semiconducting monolayers and bilayers to moderate tensile strain. The strain-induced metal-semiconductor transition is triggered by changes in the band ordering near the top of the valence band that causes an abrupt change from σ to π character of the frontier states.

DOI: 10.1103/PhysRevB.91.161404 PACS number(s): 73.20.At, 61.46.−w, 73.22.−f, 73.61.Cw

There is a growing interest in two-dimensional semiconductors with a significant fundamental band gap and a high carrier mobility. Whereas obtaining a reproducible and robust band gap has turned into an unsurmountable obstacle for graphene [1,2], the presence of heavy transition metal atoms in layered dichalcogenide compounds limits their carrier mobility [3]. Few-layer structures of layered phosphorus allotropes, such as black phosphorus, are rapidly attracting attention due to their combination of high mobility and significant band gaps [4–7]. We find it conceivable that other isoelectronic systems, such as arsenic, may display similar structural and electronic properties as few-layer phosphorene while being chemically much less reactive [8]. In this respect, the most abundant gray arsenic allotrope is the structural counterpart of the layered *A*7 or blue phosphorus [5]. Arsenic is commonly known for its toxicity, which is highest for the yellow As allotrope and should not be of concern for few-layer nanostructures. Whereas crystalline gray arsenic displays rhombohedral stacking of layers and is semimetallic [9–15], loss of crystallinity opens a fundamental band gap in the amorphous structure [10,16]. Even though few-layer gray arsenic has not been studied yet, analogies with blue phosphorene make arsenic monolayers and bilayers plausible candidates for 2D semiconductors.

Here we study the equilibrium geometry and electronic structure of thin films of layered gray arsenic using *ab initio* density functional theory. In contrast to bulk gray As that is semimetallic, thin films display a significant band gap that depends sensitively on the number of layers, in-layer strain, layer stacking, and interlayer spacing. We find that metallic character can be introduced by increasing the number of layers beyond two or by subjecting semiconducting monolayers and bilayers to moderate tensile strain. The strain-induced metal-semiconductor transition is triggered by changes in the band ordering near the top of the valence band that causes an abrupt change from σ to π character of the frontier states.

Our computational approach to gain insight into the equilibrium structure, stability, and electronic properties of arsenic structures is based on *ab initio* density functional theory as implemented in the SIESTA [17] and VASP [18] codes. We use periodic boundary conditions throughout the study, with multilayer structures represented by a periodic array of slabs separated by a vacuum region $\gtrsim$15 Å. Unless specified otherwise, we use the Perdew-Burke-Ernzerhof (PBE) [19] exchange-correlation functional for most calculations. Selected results are compared to the local density approximation (LDA) [20,21] and other functionals including the optB86b-vdW functional [22,23] that provide a better description of van der Waals interactions and the HSE06 [24,25] hybrid functional. In our SIESTA calculations we use norm-conserving Troullier-Martins pseudopotentials [26], and a double-ζ basis including polarization orbitals. The reciprocal space is sampled by a fine grid [27] of 16×16×1 k points in the Brillouin zone of the primitive unit cell for 2D structures and 16×16×3 k points for the bulk. We use a mesh cutoff energy of 180 Ry to determine the self-consistent charge density, which provides us with a precision in total energy of $\lesssim$2 meV/atom. All geometries have been optimized using the conjugate gradient method [28], until none of the residual Hellmann-Feynman forces exceeded 10^{-2} eV/Å. Equilibrium structures and energies based on SIESTA have been checked against values based on the VASP code.

In contrast to the AB-stacked isoelectronic black phosphorus, bulk gray arsenic prefers the rhombohedral (or ABC) layer stacking, with the optimized structure shown in Fig. 1. The monolayer of gray As, depicted in the top view in Fig. 1(b), resembles the honeycomb lattice of graphene with two atoms per unit cell. Unlike planar graphene, however, the unit cell is buckled, similar to blue (or *A*7) phosphorus [5], and very different from layered black phosphorus [4]. Interatomic interactions within a monolayer are covalent, resulting in a nearest-neighbor distance of 2.53 Å. The phonon spectrum of a gray arsenic monolayer, displayed in the Supplemental Material [29], shows no soft modes, thus indicating that a freestanding monolayer should be stable.

Observed and calculated structural and cohesive properties in gray arsenic are summarized in Table I. The calculated interlayer separation in the ABC-stacked bulk system is $d = 3.58$ Å, similar to the observed value [30]. The interlayer interaction energy of ≈0.02 eV/atom, based on PBE, is slightly higher than in blue phosphorus [5]. While this value is likely underestimated, the optB86b value of 0.17 eV/atom and the LDA value of 0.16 eV/atom likely overestimate

*tomanek@pa.msu.edu

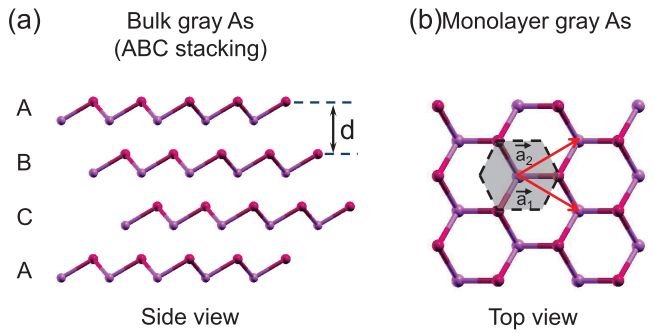

FIG. 1. (Color online) (a) Side view of the rhombohedrally (ABC) stacked layered structure of bulk gray arsenic. (b) Top view of the buckled honeycomb structure of a gray arsenic monolayer. Atoms at the top and bottom of the nonplanar layers are distinguished by color and shading and the Wigner-Seitz cell is shown by the shaded region.

the interlayer interaction, as discussed in the Supplemental Material [29]. The low interlayer interaction energy, similar to graphite and black phosphorus, suggests that few-layer As may be obtained by mechanical exfoliation from the bulk structure. The small difference in the length of the in-plane lattice vectors $a = |\vec{a}_1| = |\vec{a}_2| = 3.64$ Å in the isolated monolayer and $a = 3.85$ Å in the bulk structure can be traced back to a small difference in buckling of the layers that is introduced by the weak interlayer interaction. Changes in buckling are characterized by the pyramidalization angle [32] in the Supplemental Material [29]. In agreement with the experiment, we find AA-stacked gray arsenic to be less stable than the ABC-stacked structure, even though the energy difference lies within 10 meV/atom. The optimum interlayer separation in the less favorable AA stacking increases to $d = 5.15$ Å.

TABLE I. Observed and calculated properties of layered gray arsenic. $a = |\vec{a}_1| = |\vec{a}_2|$ is the in-plane lattice constant and d is the interlayer separation, as defined in Fig. 1. E_{coh} is the cohesive energy and E_{il} is the interlayer interaction energy per atom.

Structure	Bulk(ABC) (expt.)	Bulk(ABC) (theory)	Bulk(AA) (theory)	Monolayer (theory)
a (Å)	3.76[a]	3.85[b]	3.65[b]	3.64[b]
	–	3.85[c]	3.64[c]	3.61[c]
	–	3.82[d]	3.62[d]	3.58[d]
d (Å)	3.52[a]	3.58[b]	5.15[b]	–
	–	3.46[c]	4.20[c]	–
	–	3.47[d]	4.31[d]	–
E_{coh}	2.96[e]	2.86[b]	2.85[b]	2.84[b]
(eV/atom)	–	3.60[c]	3.53[c]	3.45[c]
E_{il}	–	0.02[b]	0.01[b]	–
(eV/atom)	–	0.16[c]	0.10[c]	–
	–	0.17[d]	0.13[d]	–

[a]Experimental data of Ref. [30].
[b]Results based on the DFT-PBE functional [19].
[c]Results based on the LDA [20].
[d]Results based on the optB86b van der Waals functional [22,23].
[e]Experimental data of Ref. [31].

In agreement with observations [10], our DFT results indicate that bulk gray arsenic is semimetallic. Our corresponding DFT results for the electronic structure of a monolayer of gray arsenic are presented in Fig. 2. In stark contrast to the bulk, the monolayer structure is semiconducting with an indirect fundamental band gap $E_g \approx 1.71$ eV. Comparison with more precise HSE06 [24,25] hybrid functional calculations, discussed in the Supplemental Material [29], indicates that the PBE value of the band gap is likely underestimated by $\gtrsim$0.4 eV in few-layer gray arsenic as a common shortcoming of DFT. Still, the electronic structure of the valence and the conduction band region in DFT is believed to closely represent experimental results. Therefore, we expect the charge density associated with frontier states near the top of the valence band, shown in Fig. 2(a), to be represented accurately. These states correspond to the energy range highlighted by the green shading in the band structure plots, which extends from midgap to 0.2 eV below the top of the valence band.

The $E(\vec{k})$ plot in Fig. 2(a) shows that states near the top of the valence band at Γ display a strong dispersion. This is a signature of a very low hole mass, caused by frontier states forming a network of σ orbitals connecting neighboring atoms, as seen in the right panel of Fig. 2(a). This is quite different from black phosphorene, where the frontier valence band states are dominated by atomic out-of-plane p orbitals with little overlap, which reduces the band dispersion and thus increases the hole mass. We find that the effective mass near Γ in few-layer arsenic is not only lower, but—in contrast to black phosphorene [4,33]—also isotropic. Since higher hole mobility values have been reported in bulk gray arsenic than in bulk black phosphorus [10], we believe that also arsenic monolayers and bilayers should display a higher hole mobility than monolayers and bilayers of black phosphorus.

As seen in Fig. 2(b), a uniform 5% in-layer compression reduces the band gap, but keeps it indirect and does not drastically change the character of the frontier states. According to Fig. 2(d), compression in excess of 10% would close the band gap, turning the monolayer metallic. Interestingly, also a uniform in-layer stretch reduces the band gap in the monolayer significantly. As seen in Fig. 2(c), stretching the monolayer by 5% moves the bottom of the conduction band near Γ. The less dispersive valence band with an energy eigenvalue −1.3 eV at Γ in the relaxed monolayer, shown in Fig. 2(a), moves up and becomes the top valence band in the stretched layer in Fig. 2(c). This band gradually flattens near Γ upon stretching the monolayer, and the system becomes a direct-gap semiconductor at tensile strain values $\gtrsim +6\%$.

More important is the change in the character of the frontier states caused by the motion of this band relative to the other valence bands near Γ. In contrast to the relaxed and compressed layer depicted in Figs. 2(a) and 2(b), the frontier states in the stretched layer are lone-pair p orbitals of tetrahedral As that are normal to the layer. The lower overlap between these atomic p orbitals is also the cause of the low dispersion of the corresponding π-like band near Γ. As we will see later, the change in character of the frontier states from σ- to π-like has a profound effect on the electronic structure near E_F in multilayer systems.

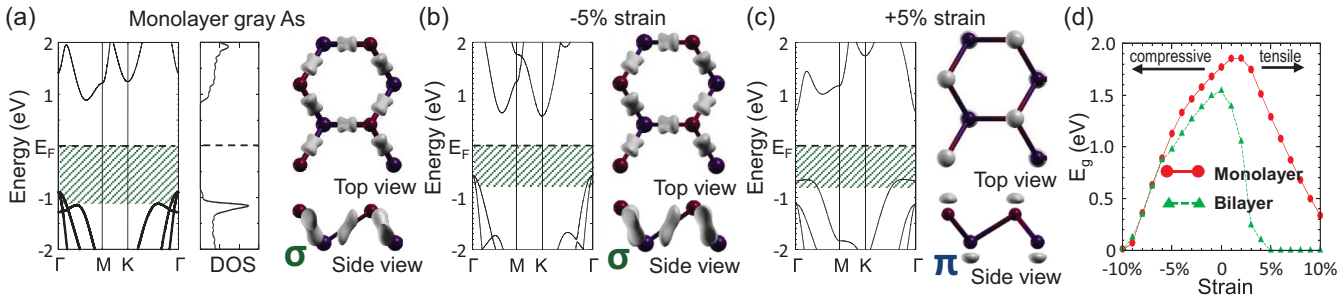

FIG. 2. (Color online) Electronic structure of (a) a relaxed monolayer of gray As, and the same monolayer subject to a uniform in-layer strain of (b) −5% and (c) +5%. The energy range between the Fermi level E_F and 0.2 eV below the top of the valence band is green shaded in the band structure in the left panels. Electron density ρ_{vb} associated with these states, superposed with a ball-and-stick model of the structure, is shown in the right panels. (d) Dependence of the fundamental band gap E_g on the in-layer strain in a monolayer and an AB-stacked bilayer of gray As.

The profound effect of the change in character of the frontier states can be seen most easily when comparing the fundamental band gap E_g in a monolayer and a bilayer in Fig. 2(d). E_g is essentially the same in both systems during compression, since the frontier states have σ character and show little overlap between layers. The character change of the frontier states to π-like upon stretching increases significantly the interlayer overlap between these states, causing a drastic reduction in E_g of the bilayer as compared to the monolayer. Quite significant in this respect is our finding that a bilayer should turn metallic for tensile strains $\gtrsim$5%. As discussed in the Supplemental Material [29], this critical tensile strain value is likely underestimated in our PBE study and is projected to increase to $\lesssim$7% according to our HSE06 calculations. We note that similar tensile strain values have been achieved experimentally on suspended graphene membranes that are more resilient to stretching due to their planar geometry [29,34–36].

A closer look at the behavior of frontier states in a bilayer subject to different levels of strain is offered in Fig. 3. As seen in Fig. 3(a), the top valence band in the relaxed bilayer has a similar low dispersion in the electronic structure near Γ as a stretched monolayer in Fig. 2(c). Also, the right panels of the two subfigures confirm the similar π character of the frontier states in a stretched monolayer and a relaxed bilayer. Since the bottom of the conduction band in the relaxed bilayer is not at Γ, the relaxed As bilayer is an indirect-gap semiconductor with a narrower gap than the relaxed monolayer.

Upon compression, the band ordering near the top of the valence band changes in the bilayer. As seen in Fig. 3(b), the frontier states in a system subject to a 5% uniform compression change their character to σ-like, similar to a compressed monolayer. The reduced overlap between frontier states on neighboring layers increases the interlayer separation d. A compressed arsenic bilayer remains an indirect-gap semiconductor.

As seen in the right panel of Fig. 3(c), a uniform +5% tensile strain in the bilayer changes the character of the frontier states to π-like, similar to our findings for the stretched monolayer reported in Fig. 2(c). The frontier states, which are primarily distributed in the interlayer region, bring the two layers closer together. The increased hybridization of interlayer frontier states at a decreased interlayer distance causes a significant band gap reduction over the monolayer subject to the same level of tensile strain. As mentioned above, the bilayer should turn semimetallic at moderate tensile strain values.

The overall dependence of the fundamental band gap on the number of layers N and the stacking sequence, depicted in Fig. 3(d), shows a uniform trend of band gap reduction with increasing value of N, which has been noted also for the different layered allotropes of phosphorus [4,5]. In particular,

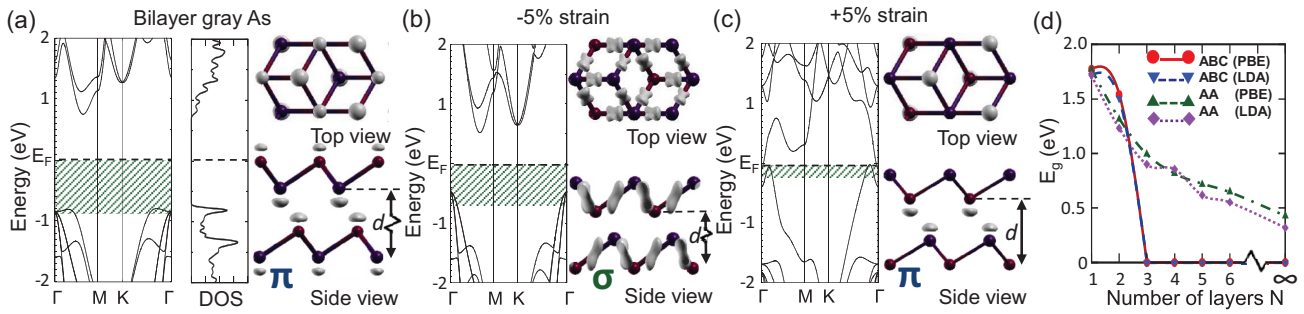

FIG. 3. (Color online) Electronic structure of (a) a relaxed AB-stacked bilayer of gray As, and the same bilayer subject to a uniform in-layer strain of (b) −5% and (c) +5%. The energy range between the Fermi level E_F and 0.2 eV below the top of the valence band is green shaded in the band structure in the left panels. Electron density ρ_{vb} associated with these states, superposed with a ball-and-stick model of the structure, is shown in the right panels. The interlayer spacing d in the side views is reduced for clarity. (d) Dependence of the fundamental band gap E_g on the number of layers N and the DFT functional in few-layer As with ABC and AA stacking. The lines in (d) are guides to the eye.

we find ABC-stacked arsenic slabs with $N > 2$ to be metallic. We also observe notable changes in the optimum interlayer distance d with changing number of layers and stacking sequence, which strongly affect the electronic structure. We find the optimum interlayer distance in AA-stacked structures to be much larger than in ABC-stacked structures, which slows down the reduction of the band gap with growing N. To check the validity of this trend, we reproduced the band gap values obtained using both PBE and LDA exchange-correlation functionals for structures optimized by PBE in Fig. 3(d). Small deviations from this trend, associated with the specific functionals, are discussed in the Supplemental Material [29].

The weak interlayer interaction in layered gray arsenic should allow for a mechanical exfoliation of monolayers and bilayers in analogy to graphene and phosphorene. More appealing for large-scale production is the reported synthesis of thin films of gray arsenic by molecular beam epitaxy (MBE) two decades ago [37], which should be also capable of producing monolayers and bilayers. Chemical vapor deposition (CVD), which had been used successfully in the past to grow graphene [38,39] and silicene [40], may become ultimately the most common approach to grow few-layer gray arsenic on specific substrates. Substrates such as Ag(111), or even Zr(0001) and Hf(0001), should be advantageous to minimize the lattice mismatch during MBE or CVD growth.

From the viewpoint of electronic applications, an ideal two-dimensional (2D) semiconductor should combine a sizable fundamental band gap with a high carrier mobility and chemical stability. Equally important is identifying a suitable way to make electrically transparent contacts. Graphene, with the exception of its vanishing band gap, satisfies the latter three criteria ideally. Transition metal dichalcogenides, including MoS_2, bring the benefit of a nonzero band gap, but display lower intrinsic carrier mobility due to enhanced electron-phonon coupling, primarily caused by the presence of heavy elements such as Mo, and suffer from high tunneling barriers at contacts to the chalcogen atoms. Few-layer systems of black phosphorus and arsenic do show a sizable band gap and the ability to form transparent contacts to metal leads. The higher carrier mobility in bulk gray As and black P over bulk MoS_2 [10] has also been observed in ultrathin black phosphorus films [4], and the same is expected for monolayers and bilayers of arsenic as well. Of the two group V elements, the heavier arsenic appears more resilient to oxidation [8]. If, indeed, gray arsenic monolayers and bilayers turn out to be chemically stable, arsenic may become an excellent contender for a new generation of 2D nanoelectronic devices.

In conclusion, we have used *ab initio* density functional theory to study the equilibrium geometry and electronic structure of thin films of layered gray arsenic. We found the PBE, LDA, and optB86b-vdW DFT functionals as well as the hybrid HSE06 functional to predict consistent trends for the interlayer distance and interaction as well as the fundamental band gap and character of the frontier states in monolayers, bilayers, and few-layer systems of gray arsenic. In contrast to bulk gray As that is semimetallic, thin films display a significant band gap that depends sensitively on the number of layers, in-layer strain, layer stacking, and interlayer spacing. We find that metallic character can be introduced by increasing the number of layers beyond two or by subjecting semiconducting monolayers and bilayers to moderate tensile strain. The strain-induced metal-semiconductor transition is triggered by changes in the band ordering near the top of the valence band that causes an abrupt change from σ to π character of the frontier states. Due to the weak interlayer interaction, gray arsenic should exfoliate easily to form few-layer structures. Alternative ways to synthesize few-layer arsenic include MBE and CVD.

We acknowledge useful discussions with Gotthard Seifert and Bilu Liu. This study was supported by the National Science Foundation Cooperative Agreement No. EEC-0832785 "NSEC: Center for High-rate Nanomanufacturing". Computational resources for this study have been provided by the Michigan State University High Performance Computing Center.

[1] M. Y. Han, B. Özyilmaz, Y. Zhang, and P. Kim, Phys. Rev. Lett. **98**, 206805 (2007).
[2] D. C. Elias, R. R. Nair, T. M. G. Mohiuddin, S. V. Morozov, P. Blake, M. P. Halsall, A. C. Ferrari, D. W. Boukhvalov, M. I. Katsnelson, A. K. Geim, and K. S. Novoselov, Science **323**, 610 (2009).
[3] M. S. Fuhrer and J. Hone, Nat. Nanotechnol. **8**, 146 (2013).
[4] H. Liu, A. T. Neal, Z. Zhu, Z. Luo, X. Xu, D. Tomanek, and P. D. Ye, ACS Nano **8**, 4033 (2014).
[5] Z. Zhu and D. Tománek, Phys. Rev. Lett. **112**, 176802 (2014).
[6] J. Guan, Z. Zhu, and D. Tománek, Phys. Rev. Lett. **113**, 046804 (2014).
[7] L. Li, Y. Yu, G. J. Ye, Q. Ge, X. Ou, H. Wu, D. Feng, X. H. Chen, and Y. Zhang, Nat. Nanotechnol. **9**, 372 (2014).
[8] N. Burford, Y.-Y. Carpenter, E. Conrad, and C. D. L. Saunders, *Biological Chemistry of Arsenic, Antimony and Bismuth* (Wiley, New York, 2010), pp. 1–17.
[9] D. Bullett, Solid State Commun. **17**, 965 (1975).
[10] O. Madelung, *Semiconductors: Data Handbook*, 3rd ed. (Springer, Berlin, 2004).
[11] J. H. Xu, E. G. Wang, C. S. Ting, and W. P. Su, Phys. Rev. B **48**, 17271 (1993).
[12] H. Tokailin, T. Takahashi, T. Sagawa, and K. Shindo, Phys. Rev. B **30**, 1765 (1984).
[13] X. Gonze, J.-P. Michenaud, and J.-P. Vigneron, Phys. Rev. B **41**, 11827 (1990).
[14] L. M. Falicov and S. Golin, Phys. Rev. **137**, A871 (1965).
[15] S. Golin, Phys. Rev. **140**, A993 (1965).
[16] M. Kelly and D. Bullett, Solid State Commun. **18**, 593 (1976).
[17] E. Artacho, E. Anglada, O. Dieguez, J. D. Gale, A. Garcia, J. Junquera, R. M. Martin, P. Ordejon, J. M. Pruneda, D. Sanchez-Portal, and J. M. Soler, J. Phys.: Condens. Matter **20**, 064208 (2008).
[18] G. Kresse and J. Furthmüller, Phys. Rev. B **54**, 11169 (1996).
[19] J. P. Perdew, K. Burke, and M. Ernzerhof, Phys. Rev. Lett. **77**, 3865 (1996).

[20] D. M. Ceperley and B. J. Alder, Phys. Rev. Lett. **45**, 566 (1980).
[21] J. P. Perdew and A. Zunger, Phys. Rev. B **23**, 5048 (1981).
[22] J. Klimeš, D. R. Bowler, and A. Michaelides, J. Phys.: Condens. Matter **22**, 022201 (2010).
[23] J. Klimeš, D. R. Bowler, and A. Michaelides, Phys. Rev. B **83**, 195131 (2011).
[24] J. Heyd, G. E. Scuseria, and M. Ernzerhof, J. Chem. Phys. **118**, 8207 (2003).
[25] A. V. Krukau, O. A. Vydrov, A. F. Izmaylov, and G. E. Scuseria, J. Chem. Phys. **125**, 224106 (2006).
[26] N. Troullier and J. L. Martins, Phys. Rev. B **43**, 1993 (1991).
[27] H. J. Monkhorst and J. D. Pack, Phys. Rev. B **13**, 5188 (1976).
[28] M. R. Hestenes and E. Stiefel, J. Res. Natl. Bur. Stand. **49**, 409 (1952).
[29] See Supplemental Material at http://link.aps.org/supplemental/10.1103/PhysRevB.91.161404 for details regarding the equilibrium structure, stability, and dependence of electronic structure results on the exchange-correlation functional used in the DFT studies.
[30] D. Schiferl and C. S. Barrett, J. Appl. Crystallogr. **2**, 30 (1969).
[31] C. Kittel, *Introduction to Solid State Physics*, 8th ed. (Wiley, Hoboken, NJ, 2004).
[32] R. C. Haddon, J. Am. Chem. Soc. **108**, 2837 (1986).
[33] R. Fei and L. Yang, Nano Lett. **14**, 2884 (2014).
[34] C. Lee, X. Wei, J. W. Kysar, and J. Hone, Science **321**, 385 (2008).
[35] I. W. Frank, D. M. Tanenbaum, A. M. van der Zande, and P. L. McEuen, J. Vac. Sci. Technol., B: Microelectron. Nanometer Struct.–Process., Meas., Phenom. **25**, 2558 (2007).
[36] M. Huang, H. Yan, T. F. Heinz, and J. Hone, Nano Lett. **10**, 4074 (2010).
[37] R. Boča, P. Hajko, L. Benco, I. Benkovský, and D. Faktor, Czech. J. Phys. **43**, 813 (1993).
[38] K. S. Kim, Y. Zhao, H. Jang, S. Y. Lee, J. M. Kim, K. S. Kim, J.-H. Ahn, P. Kim, J.-Y. Choi, and B. H. Hong, Nature **457**, 706 (2009).
[39] A. Reina, X. Jia, J. Ho, D. Nezich, H. Son, V. Bulovic, M. S. Dresselhaus, and J. Kong, Nano Lett. **9**, 30 (2009).
[40] P. Vogt, P. De Padova, C. Quaresima, J. Avila, E. Frantzeskakis, M. C. Asensio, A. Resta, B. Ealet, and G. Le Lay, Phys. Rev. Lett. **108**, 155501 (2012).